

Research Article

Dual-Band Dielectric Resonator Antenna for C and X Band Application

Deepak Batra, Sanjay Sharma, and Amit Kumar Kohli

Department of ECE, Thapar University, Patiala, Punjab 147004, India

Correspondence should be addressed to Deepak Batra, deepak.fet@mriu.edu.in

Received 27 September 2011; Revised 15 December 2011; Accepted 20 December 2011

Academic Editor: Tayeb A. Denidni

Copyright © 2012 Deepak Batra et al. This is an open access article distributed under the Creative Commons Attribution License, which permits unrestricted use, distribution, and reproduction in any medium, provided the original work is properly cited.

The proposed technique combines a slot antenna and a dielectric resonator antenna (DRA) to effectively design a dual band dielectric resonant antenna without compromising miniaturization or its efficiency. It is observed that the resonance of the slot and that of the dielectric structure merged to achieve extremely wide bandwidth over which the antenna polarization and radiation pattern are preserved. Here the effect of slot size on the radiation performance of the DRA is studied. The antenna structure is simulated using two simulators (Ansoft HFSS and CST-Studio software). The simulated results are presented and compared with the measured results. This DRA has a gain of 6 dBi and 5.5 dBi at 6.1 and 8.3 GHz, respectively, 10 dB return impedance bandwidth of nearly 4% and 6% at two resonating frequencies and 98% efficiency has been achieved from the configuration. It is shown that the size of the slot can significantly affect the radiation properties of the DRA, and there are good agreements between simulation and measured results.

1. Introduction

Modern broadband communication systems and radars require light weight compact antennas with high gain and wide bandwidth. However, Patch antennas are a popular choice for microwave electronically scanned array applications. They offer low-profile, light-weight, and low-cost solutions that can be readily integrated into microwave circuits. But the disadvantage is narrow impedance bandwidth (BW) where probe fed or proximity-coupled patch antennas are typically limited to $\sim 5\%$ BW. By using aperture-coupled patch antenna, bandwidth can be increased up to $\sim 15\%$ with moderate gain. Dielectric resonators have also received great interest in recent years for their potential applications in microwave and millimeter wave communication systems. They have been widely used as a tuning component in shielded microwave circuits such as filters, oscillators, and cavity resonators. With an appropriate feed arrangement, they can also be used as antennas, and they offer efficient radiation [1]. Dielectric resonator antennas (DRAs) in cylindrical, rectangular, and hemispherical shapes and other geometries may be used. Recently, the dielectric resonator antenna has been proposed as an alternative to the popular

microstrip patch parallel with rapid progress in microwave communication that demands miniaturization of microwave circuits. Dielectric antennas have proved themselves to be ideal candidates for antenna applications by offering several advantages, which include mechanical simplicity, very low conductor loss, large impedance bandwidth [1], and simple coupling schemes to all commonly used transmission lines [2]. Very high radiation efficiency can be smaller than conventional metal antennas and more resistant to proximity detuning when placed close to another object. DRA can be easily varied by suitably choosing the dielectric constant of the resonator material and its dimensions [3]. Dielectric resonators (DRs) are preferred because they are easy to fabricate and offer a more degree of freedom to control the resonant frequency and quality factor. However, the high Q factor restricts the bandwidth, which limits its usefulness as an antenna [4]. Therefore, high permittivity DRs are preferred in the design of antenna. Some investigations have been conducted to enhance gain of a DRA by employing offset dual-disk DRs [5, 6] and stacking parasitic DRs with an air gap between the driven and parasitic DRs, and composite-layered high-permittivity DRs.

2. Design and Simulation

To increase the usable bandwidth of a DRA, a method is demonstrated that manipulates the aspect ratio of the DRA to obtain dual-mode operation such that both modes have a VSWR less than 2.0 and similar radiation patterns.

In this work, we propose a dual band dielectric resonator antenna. By using closed form of design equations, we design aperture-coupled dielectric resonator antenna on 3D simulator. Kumar et al. suggested various techniques for optimization of bandwidth and reduction of size by proportional formulae [7, 8]. The proposed technique is mechanically stable and easy to fabricate. Here, the main concern is to obtain dual band by optimized shape and compact size of slot on ground plane in DRA system.

The layered configuration of the DRA is shown in Figure 1. The dielectric resonator, which has a dielectric constant ϵ_1 , is placed above a thin ground plane in which inductive rectangular slot inserted for matching the coupled power coming from feed line. Below ground plane is a dielectric segment with a dielectric constant of ϵ_2 . The DR has a higher permittivity than that of the dielectric segment. The DRA is excited by a feed line. This arrangement is called aperture coupled dielectric resonator antenna. The DRAs investigated here have a rectangular shape. Similarly, the dielectric segment of lower permittivity has the same surface dimension as the ground plane. The design procedure is summarized as follows.

Set $\epsilon_1 > 8 > \epsilon_2$ and estimate the initial values of the DR dimension using the dielectric waveguide model [1]

$$k_x = \frac{m\pi}{a} \left(1 + \frac{2}{ak_o\sqrt{\epsilon_r - 1}} \right), \quad (1)$$

$$k_y = \frac{n\pi}{b} \left(1 + \frac{2}{bk_o\sqrt{\epsilon_r - 1}} \right), \quad (2)$$

$$k_z = \sqrt{\epsilon_r k_o^2 - k_x^2 - k_y^2}, \quad (3)$$

$$\alpha = \frac{1}{\sqrt{(\epsilon_r - 1)k_o^2 - k_x^2}}, \quad (4)$$

$$\gamma = \frac{1}{\sqrt{(\epsilon_r - 1)k_o^2 - k_y^2}}, \quad (5)$$

where ϵ_r is permittivity of material and k_o is the free-space wave number given by

$$k_o = \frac{2\pi f_o}{c}, \quad (6)$$

where c is the speed of light in free space and f_o is the operating frequency. For well-guided modes, the fields are

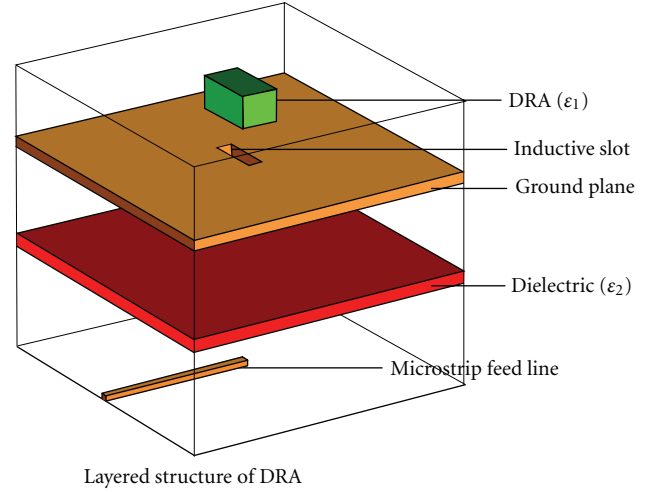


FIGURE 1: Layered structure of DRA.

confined within the guide and a further approximation can be made:

$$k_x = \frac{m\pi}{a}, \quad (7)$$

$$k_y = \frac{n\pi}{b}, \quad (8)$$

$$k_z \tan\left(\frac{k_z d}{2}\right) = \sqrt{(\epsilon_r - 1)k_o^2 - k_x^2 - k_y^2}. \quad (9)$$

This approximation is equivalent to assuming that magnetic walls exist at $x = \pm a/2$ and $y = \pm b/2$.

The value δ can be defined as the fraction of a half cycle of the field variation in the z -direction and is given by

$$\delta = \frac{k_z}{\pi/d}, \quad (10)$$

where a , b , and d represent the width, length, and height of the dielectric resonator, respectively, and the resonant frequency f_o is given by

$$f_o = \frac{c}{2\pi\sqrt{\epsilon_r}} \sqrt{k_x^2 + k_y^2 + k_z^2}. \quad (11)$$

The symbols k_x , k_y , and k_z represent the wave numbers in the x , y , and z directions, respectively. The resonance frequency of the lowest mode of the DR is set close to the lower end of the desired operating band as the starting point. Since dielectric permittivity values are fixed, the parameters length, breadth, height of DR, and height of substrate are used to determine the overall operating band of the DRA and the parameters like length and width of slot can be used for fine-tuning of operating band and/or to achieve good impedance matching within a desired band. Following this method, a rectangular DRA was designed and optimized using CST-EM STUDIO and ANSOFT HFSS software. Several commercial software packages are available for analyzing three-dimensional electromagnetic problems, which can be used to predict the input impedance with a reasonably high degree of

accuracy. These software tools are better suited for analysis than design, since the computational time can be lengthy, especially for high values of the dielectric constant. Although there are no simple equations for designing the slot dimensions of the various antenna parameters, the following guidelines can be used as a starting point for rectangular slots.

(1) The slot length l_s is chosen large enough so that sufficient coupling exists between the DRA and the feed line but small enough so that it does not resonate within the band of operation, which usually leads to a significant radiated back lobe. A good starting value is 10 mm to 21 mm. By using the formula given below, we can predict the value of l_s

$$l_s = \frac{0.4\lambda_0}{\sqrt{\epsilon_e}}, \quad (12)$$

where $\epsilon_e = (\epsilon_1 + \epsilon_2)/2$ and ϵ_1 and ϵ_2 are the dielectric constants of the DRA and substrate, respectively.

(2) A fairly narrow slot width is usually chosen to avoid a large backlobe component. A reasonable choice is $W_s = 0.2l_s$, where W_s and l_s are width and length of the slot, respectively. At high frequencies, W_s might result in a very narrow slot that may be difficult to fabricate due to etching limitations. At these frequencies, a wider slot width can be used.

In the design, the materials considered for the DR and dielectric segment are GaAs and Gil GML 1034, which have dielectric constants of 12.94 (ϵ_1) and 3.38 (ϵ_2), respectively. The dimensions of DR are $12.8 \times 7.3 \times 6.35 \text{ mm}^3$, and dimensions of slot are $W_s = 1.24 \text{ mm}$ and $l_s = 6.4 \text{ mm}$. Using the tuning and optimization functions of EM simulator, a double-band DRA is obtained.

3. Model Analysis

This section examines the dielectric waveguide model, used to estimate the resonant frequency and Q-factor for the rectangular DRA. The dielectric waveguide model was first proposed by Marcanti [9] to determine the guided wavelength in dielectric guides with rectangular cross-section. The dielectric guide is shown in Figure 2(a), having a rectangular cross-section of width a in the x -direction, height b in the y -direction, and the waves propagating in the z -direction. The field modes in the guide can be divided into TE_{mn} and TM_{mn} (where m and n denote the number of field in the x - and y -direction, resp., inside the guide). The fields within the guide are assumed to vary sinusoidally, while the fields outside the guide are assumed to decay exponentially. In order to simplify the analysis, the fields in the shaded regions of Figure 2(b) are assumed to be zero. By matching the fields at the boundary conditions, the wave propagation numbers in the x -, y -, and z -directions (k_x , k_y , and k_z) (for $|x| \leq a/2$ and $|y| \leq b/2$) and the attenuation constants in the x - and y -directions (α , γ) (for $|x| \geq a/2$ and $|y| \geq b/2$) can be determined using (1) to (11).

This approximation is equivalent to assuming that magnetic walls exist at $x = \pm a/2$ and $y = \pm b/2$. In the DRAs, to model the dielectric resonator antenna, the waveguide is truncated along the z -direction at $\pm d/2$, as shown in Figure 3(b) with

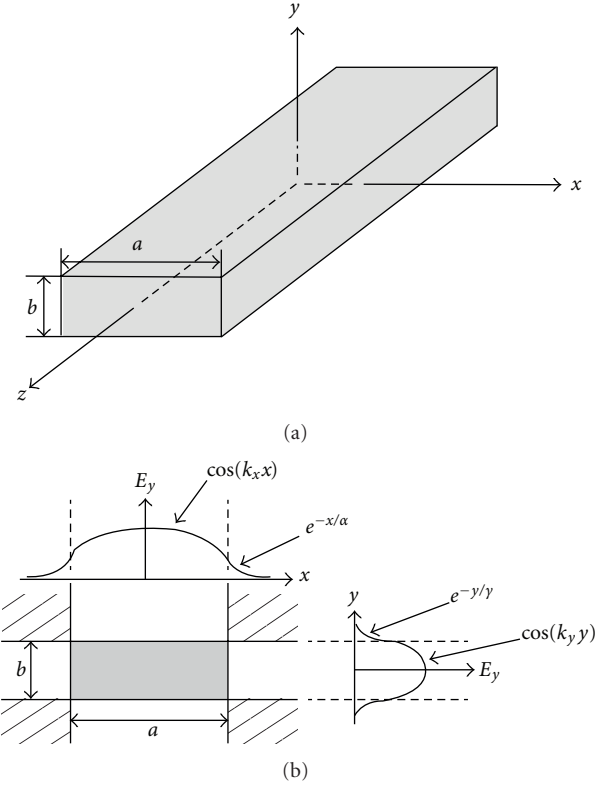


FIGURE 2: Dielectric waveguide. Adapted from [1] © 1969.

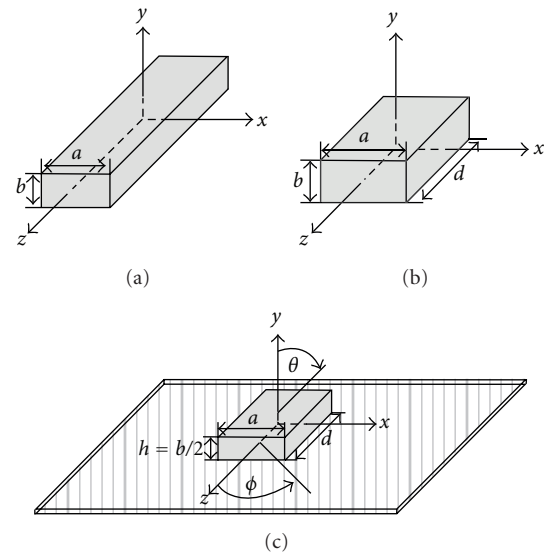


FIGURE 3: Waveguide modeled as a DRA.

magnetic walls. This model can be used for an isolated DRA in free space (with dimensions a , b , and d) or as is used in practice, for a DRA (with dimensions a , $h = b/2$, and d) mounted on a ground plane, as shown in Figure 3(c). In this latter case, image theory was used to remove the ground plane and double the height of the DRA.

For a rectangular DRA with dimensions $a, b > d$, the lowest-order mode will be $TE_{z11\delta}$. Using the dielectric waveguide model, this leads to the following fields within the DRA:

$$H_y = \frac{KyKz}{j\mu_0\omega} \cos(k_x x) \sin(k_y y) \sin(k_z z), \quad (13)$$

$$H_z = \frac{K_x^2 + K_y^2}{j\mu_0\omega} \cos(k_x x) \sin(k_y y) \sin(k_z z), \quad (14)$$

$$E_x = Ky \cos(k_x x) \sin(k_y y) \sin(k_z z), \quad (15)$$

$$E_y = -Kx \cos(k_x x) \sin(k_y y) \sin(k_z z), \quad (16)$$

$$E_z = 0, \quad (17)$$

where

$$k_x^2 + k_y^2 + k_z^2 = \epsilon_r k_0^2, \quad (18)$$

$$k_z \tan\left(\frac{k_z d}{2}\right) = \sqrt{(\epsilon_r - 1)k_0^2 - k_z^2}, \quad (19)$$

where (7) and (8) are used for k_x and k_y , respectively. To solve for the resonant frequency of the DRA, (7), (8), and (9) are first substituted into (10), and this transcendental equation is solved for k_z . The resonant frequency can then be obtained by solving for k_0 in (6), or we can directly use (11) for finding resonant frequencies for different modes. The radiation Q-factor of the DRA is determined using

$$Q = \frac{2\omega W_e}{P_{\text{rad}}}, \quad (20)$$

where W_e and P_{rad} are the stored energy and radiated power, respectively. These quantities are given by

$$W_e = \frac{abd\epsilon_r\epsilon_0}{32} \left(1 + \frac{\sin(k_z d)}{k_z d}\right) (k_x^2 + k_y^2), \quad (21)$$

$$P_{\text{rad}} = 10k_0^4 |p_m|^2, \quad (22)$$

where p_m is the magnetic dipole moment of the DRA:

$$p_m = \frac{-j\omega 8\epsilon_0 (\epsilon_r - 1)}{k_x k_y k_z} \sin\left(\frac{k_z d}{2}\right) \hat{z}. \quad (23)$$

The impedance bandwidth (BW) of the DRA can be estimated from the radiation Q-factor using:

$$\text{BW} = \frac{S - 1}{Q\sqrt{S}}, \quad (24)$$

where S is the maximum acceptable voltage standing-wave ratio (VSWR). The above equations can be used to generate the graphs for Q factors for various values of dielectric constant and various values of a/b . The normalized Q-factor is defined as

$$Q_e = \frac{Q}{\epsilon_r^{3/2}}. \quad (25)$$

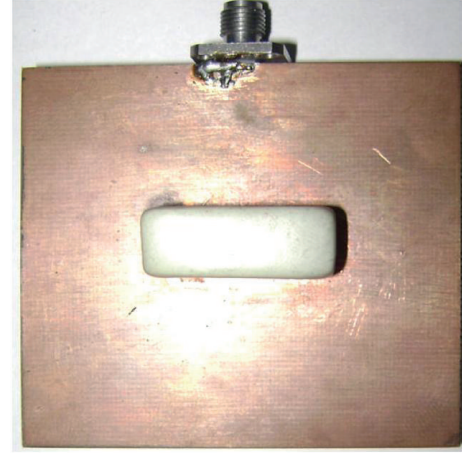


FIGURE 4: Fabricated model of aperture-coupled DRA.



FIGURE 5: Aperture feedline.

The field distribution of the lowest-order mode of the rectangular DRA, determined by the dielectric waveguide model equations, is similar to that of a short magnetic dipole. The radiation patterns generated by the DRA can, therefore, be approximated using the short magnetic dipole. The equivalent model for a rectangular DRA was mounted on an infinite ground plane and excited in the $TE_{z11\delta}$ mode. This corresponds to a horizontal magnetic dipole aligned along the z -axis. The resulting radiation patterns assume that the DRA is mounted on an infinite ground plane. For practical applications, DRAs are mounted on finite ground planes, which will have an effect on the radiation patterns due to diffraction from the edges.

4. Result and Observation

The authors observed the dual-band dielectric resonant antenna with resonant frequency 6.0 GHz and 8.3 GHz,

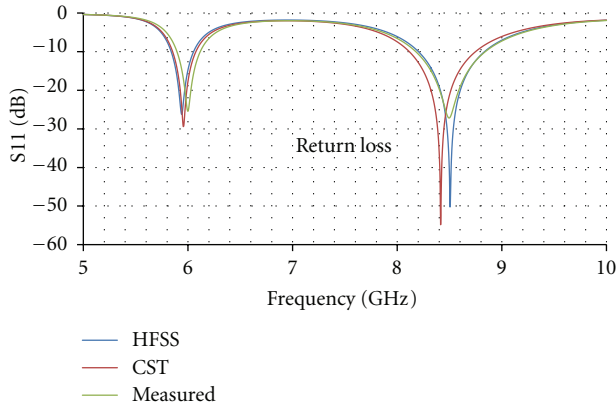


FIGURE 6: Frequency response of dual-mode DRA (near field measurement).

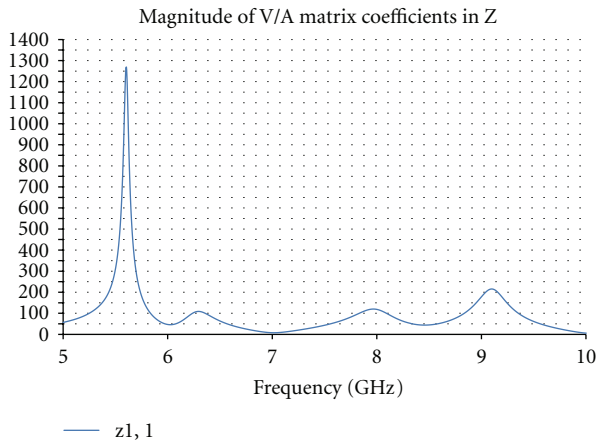


FIGURE 7: Impedance plot.

respectively. The bandwidth of each band is 280 MHz and 490 MHz, respectively. When we vary the dimension of various parameter of Dielectric Resonator (DR) and slot for optimization, we realize that the resonance frequency f_o of DRA depends on the physical dimensions of the DR and slot. The physical structure of Antenna is shown in Figures 4 and 5.

In the given Figure 6, we can see the good agreement of simulated result and measured result. At lower mode the return loss in both the cases is approximately same but at higher frequency simulated return loss is more down then measured (Figure 7).

The input impedance of antenna at resonance frequencies is approximately 50.5 ohm (Figure 8).

The measured gain is less with respect to simulated which is clearly shown in Figure 9. Simulated results in both simulators are approximately the same. The deviation of measured and simulated may be due to measurement setup.

The gain plot at both the frequencies is shown in the Figures 10 and 11.

The E-field pattern at both the frequencies is shown in Figures 12 and 13.

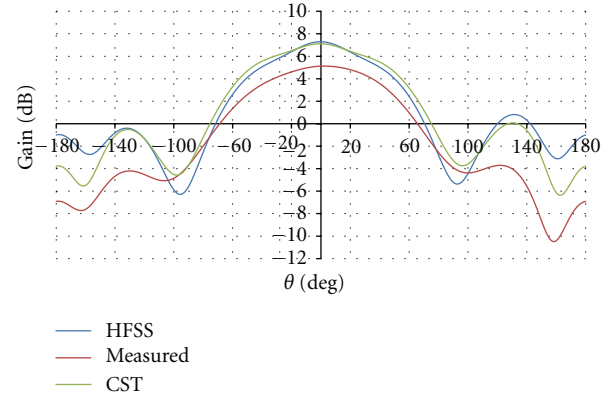


FIGURE 8: Gain plot at 6.1 GHz.

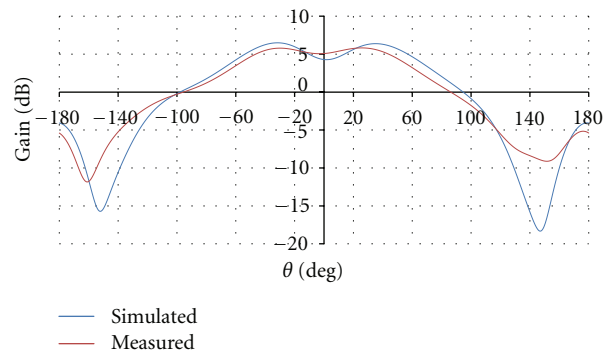


FIGURE 9: Gain plot at 8.33 GHz.

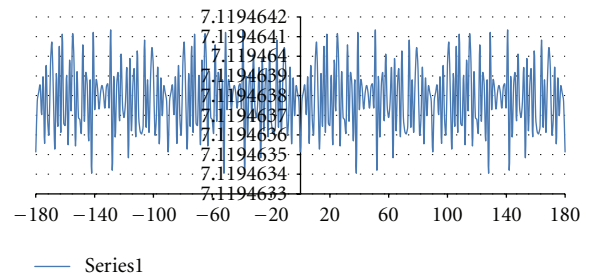


FIGURE 10: Gain plot at 6.1 GHz (phi/degree versus dB).

Figures 14 and 15 shows the H field pattern at both frequencies, 6.1 GHz & 8.3 GHz.

In Figure 16, we observed that the curve has two peaks at resonance frequency where antenna has maximum radiation performance.

We can see here the flat stable gain response over entire 6 GHz to 9 GHz as shown in Figure 17. It is an advantage of antenna in application band.

5. Conclusion

Here we have successfully designed a simple structure and compact size of dual-band low-loss aperture-coupled dielectric resonator antenna, which has almost flat stable gain

TABLE 1: Result summary.

Resonant Frequency	6.1 GHZ		8.3 GHz	
	Simulated	Measured	Simulated	Measured
Return Loss	-30 dB	-27 dB	-40 dB	-28 dB
Impedance Bandwidth	240 MHz (4%)		490 MHz (6%)	
Gain	7.1 dBi	5.9 dBi	6.3 dBi	5.5 dBi
Polarization	Linear		Slant (-30 degree)	
Beam Width	84 Degree		130 Degree	
Quality Factor	2188		3345	

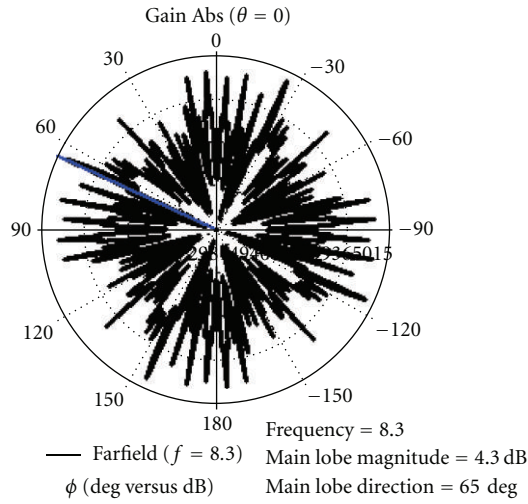


FIGURE 11: Gain plot at 8.3 GHz (phi/degree versus dB).

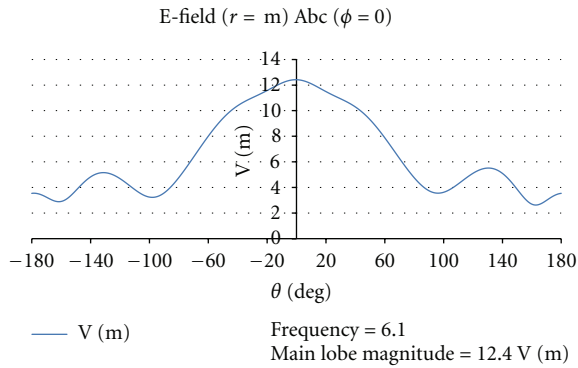


FIGURE 12: E-field pattern.

of approximately 6 dB in 6 to 9 GHz range. The antenna has high Q value as compared to conventional patch antenna whose Q is very low. Table 1 shows the values of various parameters at both the frequencies, 6.1 GHz & 8.3 GHz. Hence our designed antenna has more power handling capacity than patch antenna. This dual-band dielectric resonator antenna can find applications in C- and X-band-based communication applications such as satellite communication.

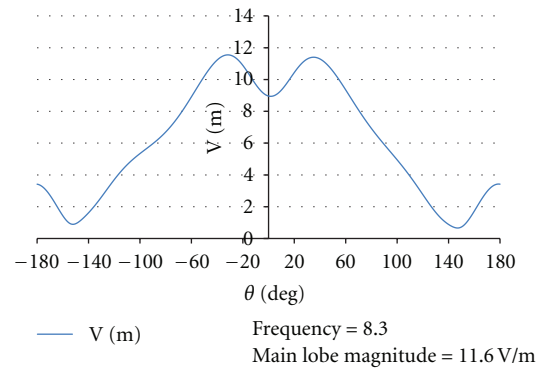


FIGURE 13: E-field pattern.

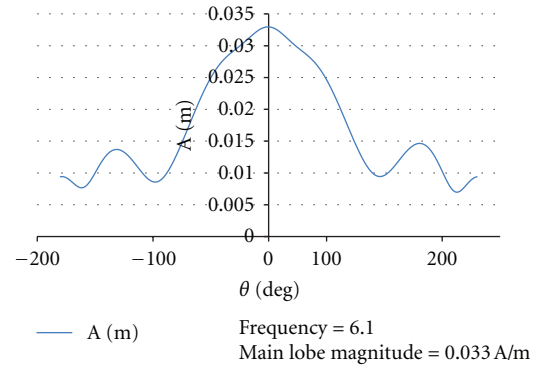


FIGURE 14: H-field pattern.

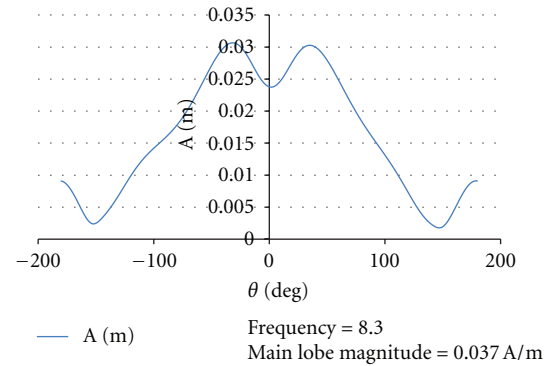


FIGURE 15: H-field pattern.

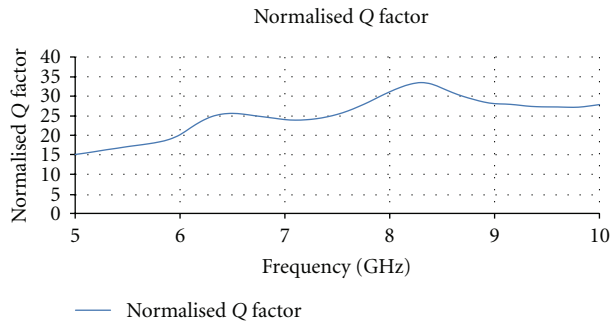


FIGURE 16: Computed normalized quality factor.

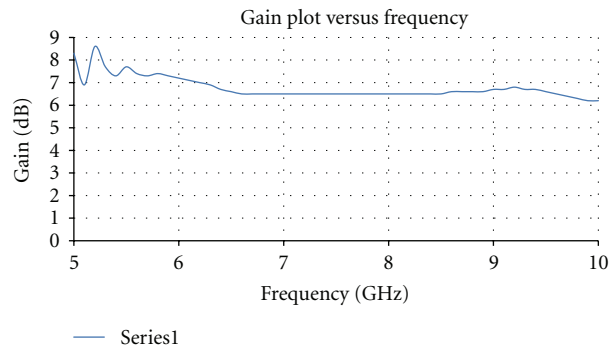


FIGURE 17: Plot of gain versus frequency.

- [6] A. Abdel Rahman, A. K. Verma, and A. S. Omar, "High gain wideband compact microstrip antenna with quasi-planner surface mount horn," in *Proceedings of the IEEE MTT-S International Microwave Symposium Digest*, vol. 1, pp. 571–574, Philadelphia, Pa, USA, June 2003.
- [7] P. Kumar, J. Kishor, and A. K. Shrivastav, "Formulation of size reduction technique in microstrip circuits by using DGS and DMS," in *Proceedings of the IEEE International Conference of Recent Advances in Microwave Theory and Applications (MICROWAVE '08)*, pp. 861–864, New Delhi, India, November 2008.
- [8] P. Kumar, R. Mahmood, J. Kishor, and A. K. Shrivastav, "Designing of a compact microstrip antenna resonating at 4.8 GHz by using size reduction technique," in *Proceedings of the International Conference on Emerging Trends in Electronic and Photonic Devices and Systems (ELECTRO '09)*, pp. 370–373, December 2009.
- [9] E. A. J. Marcatili, "Dielectric rectangular waveguide and directional coupler for integrated optics," *Bell Systems Technical Journal*, vol. 48, no. 7, pp. 2071–2102, 1969.

Acknowledgments

The authors are very thankful to Dr. A. K. Shrivastav, Program Director, SAMEER-CEM, Chennai, and Mr. Pramod kumar, Associate Professor, IPEC, Ghaziabad, for their support and guidance. They are also thankful to Antenna Division, SAMEER-CEM Chennai, for their support in simulation and measurements.

References

- [1] M. H. Neshati and Z. Wu, "Rectangular dielectric resonator antennas: theoretical modelling and experiments," in *Proceedings of the 11th International Conference on Antenna and Propagation (ICAP '01)*, vol. 480, pp. 886–870, UMIST, Manchester, UK, April 2001.
- [2] Y. M. M. Antar and Z. Fan, "Characteristics of aperture-coupled rectangular dielectric resonator antenna," *Electronics Letters*, vol. 31, no. 15, pp. 1209–1210, 1995.
- [3] D. M. Pozar, "A reciprocity method of analysis for printed slot and slot-coupled microstrip antenna," *IEEE Transactions on Antennas and Propagation*, vol. 34, no. 12, pp. 1439–1446, 1986.
- [4] D. Yau and M. V. Shuley, "Numerical analysis of an aperture coupled rectangular dielectric resonator antenna using a surface formulation and the method of moments," *IEEE proceedings of Microwave & Antenna Propagation*, vol. 146, no. 2, pp. 105–110, 1999.
- [5] K. P. Esselle, "A low-profile rectangular dielectric-resonator antenna," *IEEE Transactions on Antennas and Propagation*, vol. 44, no. 9, pp. 1296–1297, 1996.

